Modeling of the Masticatory Process with the Aid of Computer Graphic Technology

Alexander Smirnov

Institute for Computer Modelling of Biological Objects, ICMBO,
St-Peterburg, Russia
http://www.icmbo.ru
alex.smirnov.spb@mail.ru

Abstract.

Modern computer technology provides excellent opportunities to create advanced dental diagnostic and therapeutic systems, where medical products are designed using a computer-generated model. The central purpose of CAD/CAA/CAM tools for dental applications is to generate a virtual model of the dental-jaw system. The more fully and accurately the virtual model represents the mastication function, the more successful the resultant design.

This paper explores the graphic modeling of the diverse dimensionalities and topographies in the contact areas between antagonistic teeth – the occlusal fields.

Keywords: *3D reconstruction, occlusal fields, positioning of jaws models in cyberspace*

1. Introduction.

The sizes and topography of an occlusion field constantly change as the antagonistic teeth slide along the occlusal surfaces. This is known as the "occlusion process" (Fig.1).

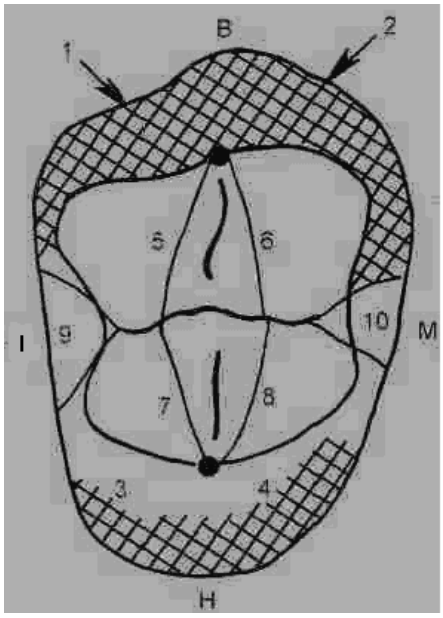

Figure 1 – Morphology of the occlusal surface of the upper right-hand bicuspid.

Note: B is the external labial surface; I is the distal surface; M is the mesial surface; H is the oral surface; 2,1 are the mesial and distal slopes of the buccal cusp; 4,3 are the mesial and distal slopes of the palatal cusp; 5,6,7,8 are the internal slopes of the cusps; 9,10 are the marginal fossae.

Between the tops of the cusps (shown in bold in Fig. 1) and the middle of the tooth there lie the triangular occlusal rims. Against these rims – or cusp ridges – the reciprocal surface of the antagonistic tooth slides. The *loci* of the sliding are shown as bold curving lines in Fig. 1. The internal slopes of cusps 5, 6, 7, 8 (Fig. 1), enclosed by the rim, are the "occlusal table." This is where the food is crushed and ground. [1, 2]

The idea, therefore, is to harness computer graphic technology in order to develop a way to model, on a polygonal grid, the geometry of the occlusal fields and the position of the point of impact of the occlusal force – the occlusion force point – at each moment of occlusion. The dimensions and topography of an occlusal field affect the force vector impacting the tooth, which, in its turn, determines the direction and extent of the micro-shifting of the tooth. Micro-shifting of the teeth impact the movement trajectory of the mandible. Therefore, knowing the trajectory of the occlusion point, we are able to model the articulatory movements more precisely.

The point of the idea is to transplant digital data about the occlusal field *loci* at specified borderline positions of the mandible, and about the geometry thereof on the original objects – the teeth, onto the polygonal grid of a three-dimensional model of the dental-jaw system. In cyberspace, further calculations of the movements of the mandible during mastication are derived from the data on the borderline *loci* of the occlusal fields according to the virtual model. [3]

On the one hand, this idea is fully sustained by the capabilities of modern computer graphic technology. On the other hand, it is fully in accord with the tenets of contemporary gnathology.

Gnathologists believe that all the functional movements of a patient's mandible can be reproduced on a high-tech 3D articulator, as long as the borderline positions are defined of the rotational centers of the condyles of the maxillo-temporal joint. [2, 4, 5] The proposed idea is exactly in line with this belief.

Since the condyles are located on the mandible, if we take any spot on the mandible, we can arguably assert that any spatial movement of that spot is associated with the movement of the condyle. In consistency with the idea we have articulated above, it is proposed, with the help of a marker, to graphically register the points of initial, maximal and final occlusal contact. The positions of the jaw, when such contacts occur, are possible when the rotational centers of the joints take specified positions in the joint. This method may be described as intraoral axiography,

as graphic record of the mandibular movement trajectory – in this case, of the borderline parts of that trajectory - is made directly on the occlusal surfaces of the teeth.

A computer system, reproducing the functional movements of the mandible in a high-tech 3D environment from intraoral axiographic data, may be defined as a "virtual articulator."

It is also important to remember that the articulation process is viewed both from the perspective of the guiding role of the maxillo-temporal joint - outside the occlusion, and from the perspective of the guiding role of the geometry of the occlusal fields – inside the occlusion.

Geometric interpretation of the object's transformation implies that, when the object's geometry changes, each representative point will move in space according to a certain trajectory, while the phase coordinates may vary within certain very small limits. If the point goes beyond the confines of acceptable values, the system will fall apart. Most of the coordinate metrics may only assume discrete values and may only be located at specified fixed points within the domain of acceptable states. [6]

2. Occlusal Field Modeling

Using the generally recognized manual manipulations [7], the dentist will, with the help of a marker, e.g. differently colored carbon paper, pinpoint the occlusal field *loci* on the teeth at the borderline occlusal positions of the mandible (Fig. 2).

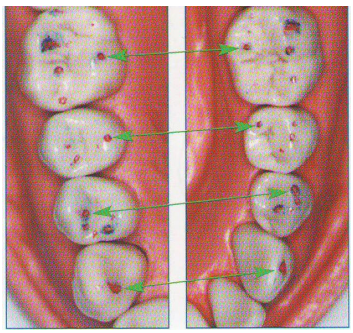

Figure 2 – Occlusal fields on the occlusal surfaces of the teeth, pinpointed by a marker (colored carbon paper).

Let's assume that the initial moment of occlusion, marked in green, corresponds to "A" localization of the occlusal fields on the occlusal surfaces of the teeth. The moment when the teeth end their movement towards the center (maximum occlusion of the teeth) is marked in blue, corresponding to "B" localization of the occlusal fields. The moment when occlusion ends (before the teeth separate) is marked in red, corresponding to "C" localization of the occlusal fields. All the three localizations may be recorded with a digital camera.

The next task is to superimpose (project) the photographic texture with the recorded localizations A, B and C of the occlusal fields onto a 3D model of the mandible (Fig. 3).

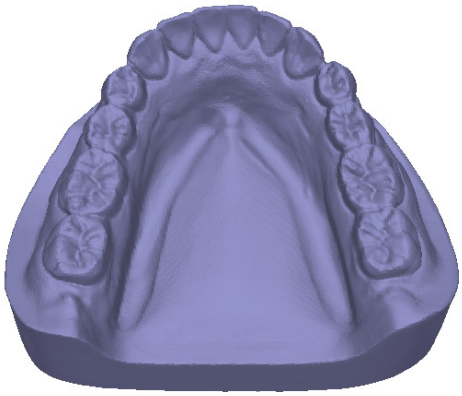

Figure 3 – 3D model of the mandible, taken from a plaster cast.

When this task is completed, we get the occlusal field localizations on a polygonal grid, representing the three borderline positions of the mandible during the occlusion process.

On a polygonal grid, the occlusal field localizations appear as relatively large sets of points, which need to be narrowed down for several reasons. First of all, the marker trace covers an accidentally colored area – a background object, as well as the physical contact area – the sought-for object. This is attested by the intensity (brightness) of the color of the trace: the color trace of the marker is more intense where the surfaces of the antagonistic teeth touch the most. Secondly, the smaller the spot, the less it is affected by large-scale distortions. Thirdly, in vector geometry, an occlusal point can only be assumed as a specified coordinate point.

Studying the occlusal field localizations A, B and C on the photograph by marker color intensity, we can identify the certain subsets a,b,c, corresponding to the occlusal fields on the virtual model. However, in the 3D environment, not all the points encompassed by subsets a, b and c will signify contact of antagonistic teeth. It is another task to identify the points of contact – occlusion points – in the subsets a,b and c.

SURF [8], the search sequence used to identify specific points in an image, was adapted as a way to accurately identify the occlusal field points. While precise identification of objects in images is a problem yet to be solved, SURF was selected from among kindred methods, because it appears to be one of the quickest and most successful sequences currently available. *Inter alia*, SURF is used in 3D reconstruction.

SURF does two things: it searches for specific points in an image and creates their descriptors, which are invariants of scale and rotation. This means that the description of a critical point will remain the same even if the size of the specimen changes, or if the specimen is

rotated (meaning rotation on the picture plane). Furthermore, the search itself for the critical points also has to possess the properties of an invariant, so that when the “scene object” is turned, it will still have the same set of critical points as the specimen.

Let us, first of all, identify the critical points and small areas around them on the specimen. At the core of the identification of specific points with SURF is calculation of the Hessian Matrix determinant (the Hessian).

The Hessian Matrix for a two-dimensional function, and its determinant, are defined as follows [9]:

$$H(f(x,y)) = \begin{bmatrix} \frac{\partial^2 f}{\partial x^2} & \frac{\partial^2 f}{\partial x \partial y} \\ \frac{\partial^2 f}{\partial x \partial y} & \frac{\partial^2 f}{\partial y^2} \end{bmatrix} \tag{1}$$

This is what the definition a Hessian Matrix determinant looks like:

$$det(H) = \frac{\partial^2 f}{\partial x^2}\frac{\partial^2 f}{\partial y^2} - \left(\frac{\partial^2 f}{\partial x \partial y}\right)^2 \tag{2}$$

The Hessian Matrix determinant (the Hessian) reaches its extremes at the points of maximum change of the brightness gradient, which means that the Hessian value helps to identify the local minimum or maximum color brightness. The method detects spots pretty well [10] (Fig.3).

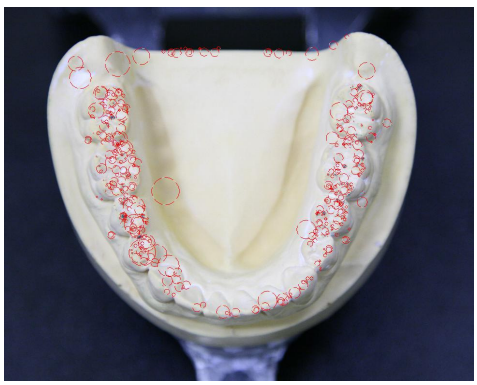

Figure 3 – Critical points found with the aid of the Hessian Matrix

Note: in this experiment, the tests were performed on a photograph of some plaster molds of human jaws.

For every critical point, we calculate the direction of maximum brightness change (the gradient) and the scale, taken from the scale ratio of the Hessian Matrix. An integral presentation of images is used for better results in calculating the Hessian filter. Integral presentation is a

matrix, the dimensionalities of which match the dimensionalities of the source image, and the elements of which are calculated according to this formula:

$$II(x,y) = \sum_{i=0,j=0}^{i\leq x, j\leq y} I(i,j) \quad (3)$$

where I(i,j)is the pixel brightness of the source image. [9]

Each element of matrix II[x,y] is the sum of the pixels in the rectangle from (0,0) to (x,y). Matrix calculation takes a length of linear time in proportion to the number of pixels in the image. With an integral matrix, it is easy to compute the sums of pixel brightnesses in arbitrary rectangular parts of the image, according to this formula:

SumOfRect(ABCD) = II(A) + II(C) — II(B) — II(D) (4)

where ABCD is the rectangle we are interested in. [9]

Once the critical points are identified, SURF will generate their descriptors. A descriptor is a set of 64(or 128) digits for every critical point. These digits represent fluctuation of the gradient around the critical point. Given that a critical point represents the maximum Hessian value, this is a guarantee that there must be areas with different gradients in the vicinity of the point – thus the dispersion (variance) of descriptors is assured for the different critical points. [9]

Therefore, when the sequence is set to work, it will identify the extremes of the determinant within the space of the scale and of the coordinates. The extreme values thus identified are then interpolated with sub-pixel precision by both coordinates and scale, resulting in accurate detection of the positions and sizes of the occlusal fields. (Fig. 4).

Figure 4 – Occlusal fields after the filter.

Now the photo texture, on which the *loci* of the occlusal fields are identified, is ready to be projected onto a three-dimensional model.

3. Positioning of Maxillary and Mandible Models in Cyberspace.

At the outset, we have specific sets of points in a 3D environment on our models of the upper and lower jaws. We assume rigidity for all the points of the sets corresponding to the occlusal fields:

The pairs of contacting occlusal fields in certain positions of the lower jaw are represented by the following correspondences (Fig.5):

$M_1(a^1{}_1a^2{}_1)$,… $M_n(a^1{}_na^2{}_n)$ are correspondences for the position when occlusion begins;

$N_1(b^1{}_1b^2{}_1)$,… $N_n(b^1{}_nb^2{}_n)$ are correspondences for the position of maximum occlusion (bite);

$L_1(c^1{}_1c^2{}_1)$,… $L_n(c^1{}_nc^2{}_n)$ are correspondences for the position at the end of occlusion,

where M, N, L signify correspondences in specific positions, the subscript index is the number of the correspondence, superscript index ^{1} signifies the upper jaw, index ^{2} the lower jaw.

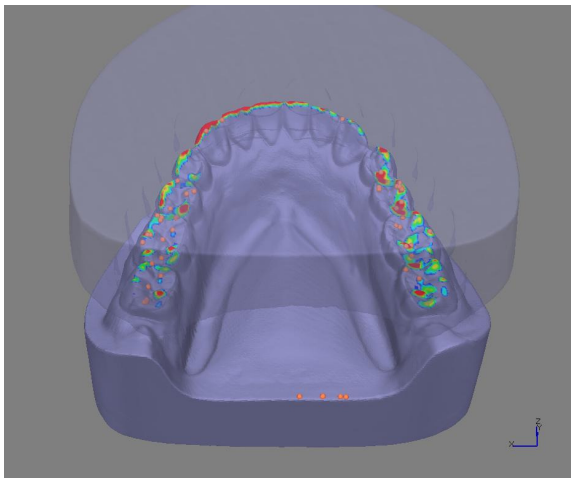

Figure 5 – Occlusal fields.

Note: green areas are the fields of the beginning of occlusion, blue are the fields of maximum occlusion, and red are the fields of the end of occlusion.

To initially combine antagonistic jaws in cyberspace, it is sufficient to study the occlusal fields of the N correspondences (correspondences in the position of the bite). The acceptable transformations in this operation are rotation or transfer in the 3D environment. We do not know which points in the N correspondences signify contact between antagonistic fields in the transformations of the preset class.

Therefore, the task of combining the antagonistic jaws comes down to finding such a transformation in the preset class, under which in certain three N correspondences, specific

points will come into contact with each other the maximum number of times in all the possible transformations.

The search for specific points – or occlusion points in bite position – looks like sorting through the points of the N correspondences in all their possible transformations according to the preset class. In a way, it reminds one of the RANSAC method. RANSAC is considered a reliable method of evaluating the metrics of a model by random sampling. The RANSAC sequence is resilient to pollution in the source data. [11, 12]

Source data set *X* enters the sequence at input. Function *M* computes metrics θ of model *P* by the data set received from *n* points. Evaluator *E* identifies correspondences between points in the resultant model. The evaluation function is subject to threshold value *t*.

The whole sequence is a single cycle, in which every iteration *k* may logically be viewed as two stages.

Stage one is the choice of points and computation of the model. From set *X* of the source points, an "n" of different points are randomly selected. Using the selected points, we calculate metrics θ of model *P* with the aid of function *M*. It is customary to refer to a constructed model as "hypothesis."

Stage two: testing the hypothesis. We test how well each point corresponds to our hypothesis with the help of evaluator *E* and threshold *t*. We mark each point as an "inlier" ("pertinent") or "outlier" ("rejected"). When all the points have been tested, we need to see whether this hypothesis is the best there is at present, and if it is, then it will supersede the foregoing best hypothesis.

At the end of the work, the latest best hypothesis will remain.

At the output of this method, we have: metrics θ of model *P* and the source data points, marked as "inliers" or "outliers."

In our case, the selection criterion is the number of the point's contacts in all of its possible transformations.

Fig. 6 shows the result of the sequence that combines maxillary models in cyberspace in the bite position.

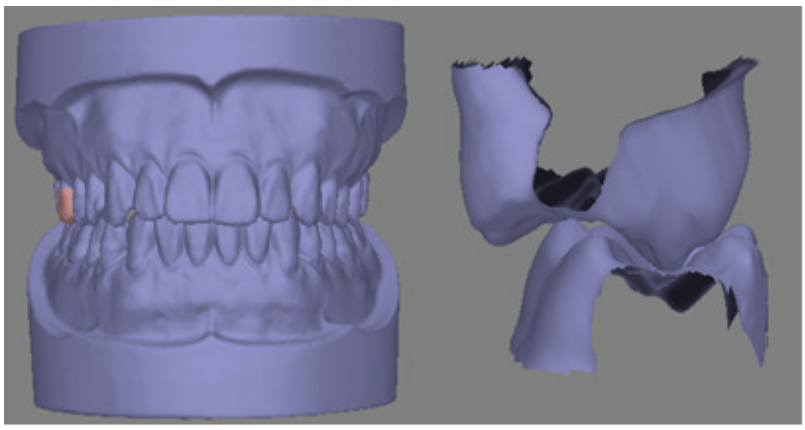

A B

Figure 6 – Visualization of central occlusion (bite position).

Note: A is the frontal view: on the right (the sides are marked as on a patient), a pair of antagonistic teeth are marked: the upper 16^{th} and lower 46^{th} (teeth are numbered according to the international FDI chart); B are the antagonistic teeth 16 and 46 with multiple cusp-and-fissure contact (a fissure is a crack or a fossa).

This sequence also applies to the M and L correspondences.

Fig.7, 8 show the result of the sequence that combines maxillary models in M correspondences.

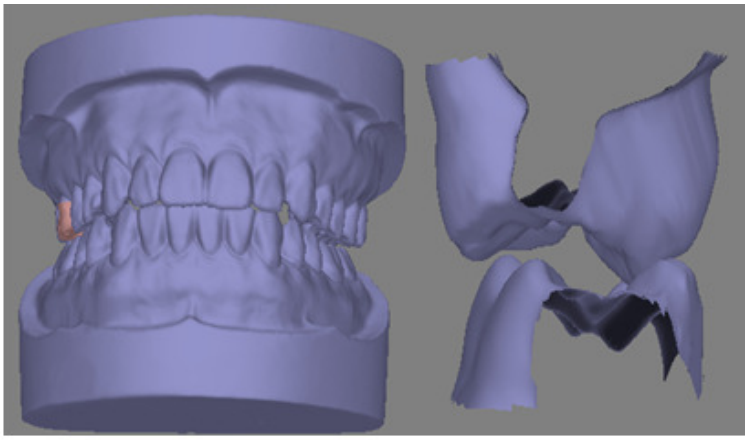

A B

Figure 7 – Visualization of primary maxillary contact during the masticatory process (beginning of occlusion), right is the working side.

Note: A is the frontal view; B are the antagonistic teeth 16 and 46: contact occurs between the palatal cusps of the upper tooth and buccal cusps of the lower.

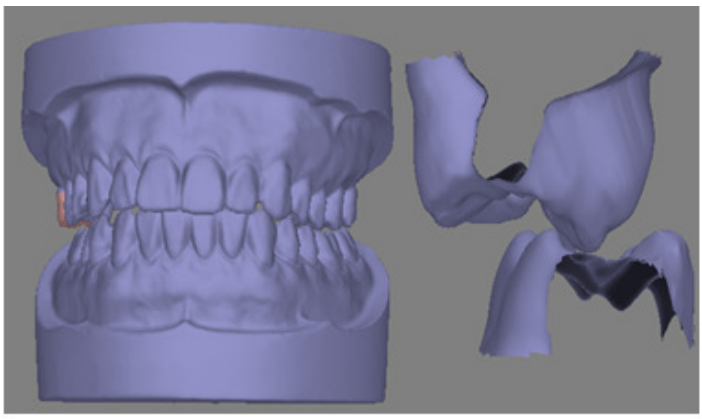

A B

Figure 8 – Visualization of primary maxillary contact during the masticatory process (beginning of occlusion), left is the working side.

Note: A is the frontal view; B are the antagonistic teeth 16 and 46: contact occurs between the palatal cusps of the upper tooth and buccal cusps of the lower.

Fig. 9 shows the result of the sequence that combines maxillary models in L correspondences.

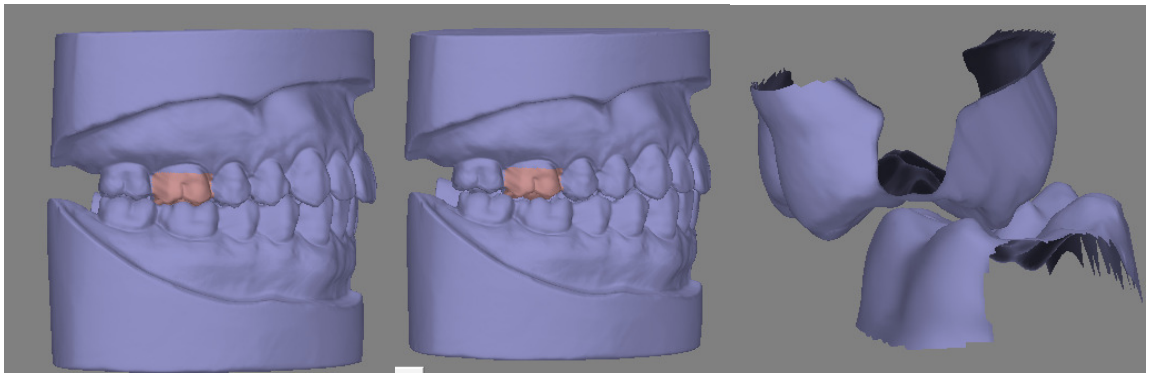

A B C

Figure 9 – Visualization of the end of occlusion.

Note: A is the lateral view from the right in the bite position; B: the lower jaw is shifted forward a little from the bite position; C are the antagonistic teeth 16 and 46 in contact before the rows of teeth separate (end of occlusion).

4. Modeling of the Occlusion Point Trajectory.

Next we proceed to model the trajectory of the occlusion point. Knowing the occlusion point trajectory, we will be able to determine the point of force application to the tooth at any moment of occlusion and, therefore, we can compute the direction and extent of the micro-shift of the tooth at any moment of occlusion.

The occlusion point trajectory is modeled on the surface of a rigid object, taking into account the chart of surface elevations. For any tooth, the trajectory begins at the occlusion point in set

“a”, from where the trajectory model follows the shortcut to the occlusion point in set “b”, and then takes another shortcut to the occlusion point in set “c”.

In a sense, this sequence is a logical segue to the previous one. This maxillary combination sequence identifies not only the thought-after transformation, but also certain specific points in certain three N correspondences, which are the occlusion points in those particular correspondences. The occlusion points in the other N correspondences are identified *ex post* on the model. In the end, we obtain the coordinates of all the occlusion points in all the “b” sets.

When we apply the maxillary combination sequence to the M and L correspondences, we obtain the occlusion point coordinates in all the “a” and “c” sets.

The occlusion point trajectories for the sections ab & bc will follow the shortest distances between the occlusion points in those sets. However, trajectories run on surfaces with some terrain. Consequently, an occlusion point trajectory will appear as a curving line in the 3D environment (Fig.10).

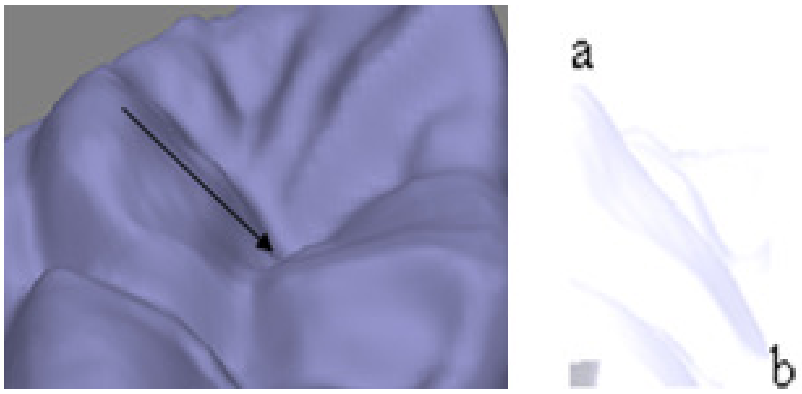

A B

Figure 10 – Section of an occlusal surface in the vicinity of the occlusion point trajectory in section “ab”

Note: A – the arrow shows the shortest distance between the occlusion point positions in set “a” (beginning of occlusion) and set “b” (maximum occlusion); B is tooth surface terrain in the trajectory section “ab”.

5. Conclusion.

We must admit that the methods, brought to your attention here, come with certain assumptions and limitations.

The sequence that determines the occlusion point trajectory accounts for the occlusive surface topography (terrain), and the localization of the borderline positions of the occlusion points; however, it assumes that the movement of the occlusion points in sections “ab” and “bc” follows the shortest way. This assumption is explained by the fact that, so far, for the purposes of intraoral axiography there exist no optimal techniques of manual manipulation in the oral cavity

and no fully reliable markers that would inform an upgrade from the mere identification of the borderline parts of the occlusion point trajectory to a full graphic description of the trajectory line on the teeth.

The above assumption imposes certain limitations on the reproduction of the occlusal processes in a virtual model, but this is not a fatal flaw. It can be easily overcome as digital data collection technology becomes more sophisticated (e.g. through the application of electronic instruments similar to “Arcus Digma” for extraoral axiography). The prospects look good, particularly since the inclusion in specialized dental CAD/CAA/CAM systems of instruments detecting various physical phenomena is in perfect harmony with the ultimate purpose: to reconstruct complex, highly nuanced processes with the aid of IBR techniques.

6. References.

[1] Hohmann A., Hielscher W., Lehrbuch der Zahntechnik. – Berlin: Quintessenz. – 1993. – Bd 1. – 487s.

[2] Хватова В.А. Клиническая гнатология./В.А.Хватова. - М.: ОАО «Издательство «Медицина», 2005. - 296 с.

[3] Смирнов А.Г., Пат. 80111 Российская Федерация, МПК A61C 7/00. Программно-аппаратная система функционального анализа окклюзии и артикуляции № 2008138078/22; заявл. 24.09.2008 ; опубл. 27.01.2009, Бюл. № 3.

[4] Насибуллин Г.Г. Центральная окклюзия, прикус и височно-нижнечелюстной сустав//Труды VII Всесоюзного съезда стоматологов. – М., 1981. – С. 287-291.

[5] Becker G.M., Kaiser D.A. Evolution of Occlusion and Occlusal Instruments//J.Prosthodont. – 1993. – Vol. 2, N 1. – P. 33-34.

[6] Андерсон Джеймс. Дискретная математика и комбинаторика (Discrete Mathematics with Combinatorics). — М.: «Вильямс», 2006. – С.960.

[7] Klineberg I., Jagger R. G.: Occlusion and Clinical Practice: An Evidence-Based Approach, p. 160 ISBN-10 0723610924

[8] Speeded-Up Robust Features (SURF). Herbert Bay, Andreas Ess, Tinne Tuytelaars, and Luc Van Gool . ftp://ftp.vision.ee.ethz.ch/publications/articles/eth_biwi_00517.pdf

[9] Crow, Franklin. “Summed-area tables for texture mapping”. SIGGRAPH '84: Proceedings of the 11th annual conference on Computer graphics and interactive techniques. pp. 207–212.

[10] Кудрявцев Л.Д. Краткий курс математического анализа. Т.2. Дифференциальное и интегральное исчисления функций многих переменных. Гармонический анализ. ФИЗМАТЛИТ, 2002, — 424 с.

[11] Martin A. Fischler and Robert C. Bolles (June 1981). «Random Sample Consensus: A Paradigm for Model Fitting with Applications to Image Analysis and Automated Cartography». Comm. Of the ACM 24: 381–395.
[12] P.H.S. Torr, and D.W. Murray (1997). «The Development and Comparison of Robust Methods for Estimating the Fundamental Matrix». International Journal of Computer Vision 24: 271–300.